Genetic dissection of theta rhythm heterogeneity in mice

Jonghan Shin*, Daesoo Kim*†, Riccardo Bianchi‡, Robert K. S. Wong‡, and Hee-Sup Shin*§

*Division of Life Sciences, Korea Institute of Science and Technology, Seoul 136-791, Korea; and ‡Department of Physiology and Pharmacology, State University of New York Health Science Center, Brooklyn, NY 11203

Edited by Nancy J. Kopell, Boston University, Boston, MA, and approved October 20, 2005 (received for review July 7, 2005)

Rhythmic oscillatory activities at the theta frequency (4–12Hz) in the hippocampus have long-attracted attention because they have been implicated in diverse brain functions, including spatial cognition. Although studies based on pharmacology and lesion experiments suggested heterogeneity of these rhythms and their behavioral correlates, controversies are abundant on these issues. Here we show that mice harboring a phospholipase C (PLC)-$\beta1^{-/-}$ mutation (PLC-$\beta1^{-/-}$ mice) lack one subset of theta rhythms normally observed during urethane anesthesia, alert immobility, and passive whole-body rotation. In contrast, the other subset of theta rhythms observed during walking or running was intact in these mutant mice. PLC-$\beta1^{-/-}$ mice also have somewhat disrupted theta activity during paradoxical sleep but do have an atropine-resistant component of theta rhythm. In addition, carbachol-induced oscillations were obliterated in hippocampal slices of PLC-$\beta1^{-/-}$ mice. Interestingly, PLC-$\beta1^{-/-}$ mice showed deficits in a hidden platform version of the Morris water maze yet performed well in motor coordination tests and a visual platform version of the Morris water maze. The results genetically define the existence of at least two subtypes of theta rhythms and reveal their association with different behaviors.

cognition | behavior | metabotropic glutamate receptor | muscarinic receptor | phospholipase C

Hippocampal theta rhythms (4–12 Hz) in rodents and humans have been implicated in diverse cognitive and behavioral functions, including arousal, attention, voluntary movement, learning, memory, sensorimotor integration, and spatial cognition (1–11). However, controversy surrounding hippocampal theta rhythm heterogeneity has prevented study of the underlying molecular and cellular mechanisms and their role in cognition and behavior (3). It has been suggested that hippocampal theta rhythms can be classified into two subgroups based on their pharmacological sensitivity: atropine-sensitive and atropine-resistant (1–3, 11–14). The former is abolished by an injection of muscarinic antagonists (e.g., atropine or scopolamine) into the animal, whereas the latter is relatively unaffected by the same drugs (for review, see ref. 1). In contrast, it has been suggested that the hippocampal theta rhythm is unitary and that the dualistic theory of hippocampal theta rhythm resulted from confounding modulatory effects on the unitary theta rhythm by muscarinic antagonists. For example, anticholinergics (e.g., atropine and scopolamine) may penetrate the brain poorly and may not totally block central cholinergic synapses, and a highly activated reticuloseptohippocampal system may drive theta during walking by overriding the partially saturated hippocampal cholinergic receptors (for review, see ref. 13 and ref. 15). In contrast, a recent *in vitro* study (16) showed that activation of group I metabotropic glutamate receptors (mGluRs) in hippocampal slices could generate atropine-resistant theta rhythm, a finding incompatible with the traditional hypothesis that the pacemaker of atropine-resistant component of hippocampal theta rhythm is located outside the hippocampus (1, 3, 11–13, 17). Therefore, further studies are needed to clarify these critical issues regarding the heterogeneity of theta rhythms in the hippocampus.

Phosphoinositide-specific phospholipase C (PLC) hydrolyses phosphatidylinositol 4,5-bisphosphate and produces a pair of second messengers: diacylglycerol and inositol 1,4,5-trisphosphate (IP_3) (18). Diacylglycerol stimulates PKC, which phosphorylates various substrate proteins and enzymes regulating neural development, neurotransmitter release, receptor and ion channel activities, and synaptic plasticity, whereas IP_3 mobilizes Ca^{2+} from intracellular stores via the intracellular IP_3 receptors (19). PLC-β is one of the three subtypes of PLC and is distinguished from PLC-γ and PLC-δ by structure and activation mechanisms. PLC-β acts through G protein-dependent pathways, and the G_q/PLC-β pathway is engaged by the activation of specific isoforms of hormone and neurotransmitter receptors that have seven transmembrane segments, e.g., mGluR1 and mGluR5 (20), and by the M1, M3, and M5 muscarinic acetylcholine receptors (21). Protein purification and molecular cloning have identified four PLC-β isoforms: PLC-β1, PLC-β2, PLC-β3, and PLC-β4 (22). Interestingly, each PLC-β isoenzyme has a unique distribution pattern in the brain (23). PLC-β2 is distributed in the white matter, suggesting its expression in nonneuronal cells; expression of PLC-β3 is low throughout the brain; expression of PLC-β4 is highly expressed in the medial septum and is almost negligible in the hippocampus; and PLC-β1 is highly expressed in the hippocampus but not detectable in the medial septum (24). PLC-β1 is the most critical isoenzyme among four PLC-β isoenzymes in studies of the hippocampal theta rhythm heterogeneity because (*i*) it is coupled not only to muscarinic receptors (23) but also to group I mGluRs in the hippocampus (25) and (*ii*) it is highly expressed in the hippocampus within the septohippocampal network, which is known to be critically involved in the generation of hippocampal theta rhythms (1, 3, 5, 10–13).

Here, we analyzed the knockout mice for the PLC-β1 gene (PLC-$\beta1^{-/-}$ mice) (23), focusing on the generation of theta rhythms in association with diverse behaviors. The results provide genetic evidence for theta rhythm heterogeneity and present their potential behavioral correlates.

Materials and Methods

Animals. F1 homozygous mice and wild-type littermates were obtained by crossing C57BL/6J(N8)PLC-$\beta1^{+/-}$ and 129S4/SvJae(N8)PLC-$\beta1^{+/-}$ mice. The genotypes were determined by using PCR analyses as described in ref. 23. Animal care and handling followed institutional guidelines (the Korea Institute of Science and Technology and the State University of New York Health Science Center). Mice were maintained with free access to

Conflict of interest statement: No conflicts declared.

This paper was submitted directly (Track II) to the PNAS office.

Freely available online through the PNAS open access option.

Abbreviations: mGluR, metabotropic glutamate receptor; PLC, phospholipase C; EEG, electroencephalogram; EMG, electromyogram.

†Present address: Department of Life Sciences, Korea Advanced Institute of Science and Technology, Daejeon 305-701, Korea.

§To whom correspondence should be addressed at: Center for Neural Science, Division of Life Sciences, Korea Institute of Science and Technology, P.O. Box 131, Cheongryang, Seoul 130-650, Korea. E-mail: shin@kist.re.kr.

food and water under a 12-h light/dark cycle with light beginning at 6:00 a.m.

Intracellular Recording in Hippocampal Slices. Transverse 400-μm-thick slices were prepared in oxygenated cold artificial cerebrospinal fluid (126 mM NaCl/5 mM KCl/2 mM $CaCl_2$/1.6 mM $MgCl_2$/26 mM $NaHCO_3$/10 mM dextrose at pH 7.4) and placed at an interface of air and artificial cerebrospinal fluid in a warm, humidified (33°C with 95% O_2/5% CO_2) recording chamber. Hippocampal slices were obtained from 64 wild-type (PLC-$\beta1^{+/+}$) and 47 mutant (PLC-$\beta1^{-/-}$) mice 2–3 weeks of age and from four wild-type and three mutant mice 3–8 weeks of age. Intracellular recordings were performed by using electrodes (40–60 MΩ) filled with 2 M potassium acetate in cells showing a stable resting membrane potential less than −55 mV. Signals were amplified with a high-impedance amplifier that allowed for capacitance compensation and for current injection through the recording electrode using an active bridge (AxoClamp-2a; Axon Instruments, Foster City, CA). Data analysis software included PCLAMP and AXOSCOPE (Axon Instruments) and SIGMAPLOT (SPSS, Chicago).

Field Recordings *in Vivo*. Male PLC-$\beta1^{-/-}$ mice 10- to 14-weeks of age and wild-type littermates were prepared for recording hippocampal electroencephalogram (EEG) signals. The experimenter was blind to the genotypes of the mice. Recordings were done according to published protocols (2) with some modifications. Briefly, for electrode implantation, the animals were anaesthetized with pentobarbital (50 ml/kg i.p.) and held in a stereotaxic apparatus with bregma and lambda in the same horizontal plane. Hippocampal EEG recordings were performed with Teflon-coated tungsten electrodes (150 μm) implanted in the hippocampal fissure (from Bregma, 2.0 mm anteroposterior, 1.2 mm mediolateral, and 1.8 mm dorsoventral) with grounding over the cerebellum. Field potential was recorded after being amplified (×1,000), bandpass-filtered (0.1–100 Hz), digitized with 12-bit resolution continuously at 1-kHz sampling, and recorded on a personal computer. For electromyogram (EMG) recording, a Teflon-coated tungsten electrode was inserted into the nuchal musculature and grounded with a wound clip for the suture. EMG signal was amplified (×1,000), bandpass-filtered (10–100 Hz), digitized with 12-bit resolution continuously at 1-kHz sampling, and recorded on a personal computer. EEG and EMG data were analyzed offline. The position of the electrodes was verified by light microscopy in the Nissl-stained sections according to published protocols (2). For detailed methodology and data analysis, see *Supporting Text*, which is published as supporting information on the PNAS web site.

Behavioral Tests. Behavioral tests were performed on male PLC-$\beta1^{-/-}$ mice and wild-type littermates aged 10–20 weeks, and the data were analyzed in a double-blind fashion. Two behavioral tests (rotating rod test, and Morris water maze) were conducted (for details, see *Supporting Text*).

Statistical Analysis. Differences between groups were compared with Student's *t* test after confirming that data sets were normally distributed. Differences between behavioral data for the mutant and wild-type mice were analyzed by repeated-measure ANOVA followed by Tukey's post hoc test (SAS Version 8, SAS Institute, Cary, NC) to analyze the data for differences between genotypes.

Results

Rederivation of PLC-$\beta1^{-/-}$ Mutation. Previously reported PLC-$\beta1^{-/-}$ mutant mice developed severe seizures, showed retarded growth, and suffered from early death (23), limiting their usefulness in behavioral studies. By controlling the genetic background through breeding, for the present study we derived PLC-$\beta1^{-/-}$ mice that were free from such complications (for details, see *Supporting Text* and Fig. 7, which is published as supporting information on the PNAS web site).

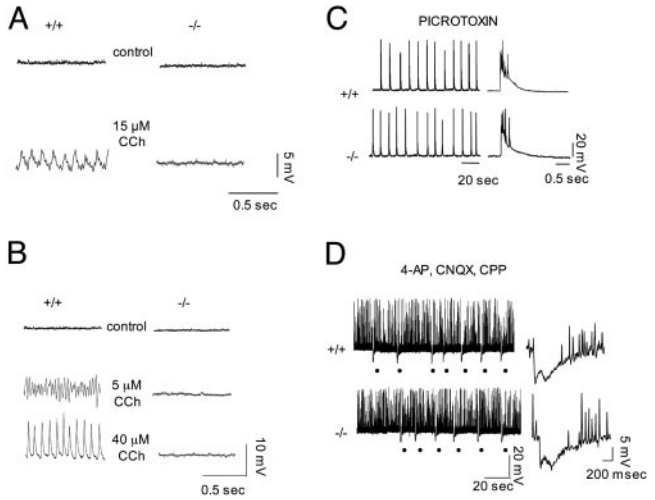

Fig. 1. Lack of carbachol-induced oscillations in the PLC-$\beta1^{-/-}$ hippocampal slices. (*A*) Carbachol (CCh) at 15 μM induced 9-Hz population oscillations in a CA3 pyramidal cell of a wild-type preparation (+/+). No oscillations were observed in a PLC-$\beta1^{-/-}$ slice preparation 1 h after carbachol treatment (−/−). (*B*) Changes in carbachol dosage modulated the frequency characteristics of carbachol-induced oscillations in wild-type slices. The peak frequencies obtained at 5 and 40 μM carbachol concentrations are ≈12 and 30 Hz, respectively. In contrast, in the PLC-$\beta1^{-/-}$ slices, no oscillatory activity was generated by different concentrations of CCh. (*A* and *B*) The membrane potential throughout the records shown was maintained close to −70 mV. (*C*) Picrotoxin-induced synchronized bursts in CA3 pyramidal cells in PLC-$\beta1^{+/+}$ and PLC-$\beta1^{-/-}$ slices recorded 1 h after addition of picrotoxin (50 μM). The bursts are displayed on two different time scales and represent synchronized population activity because they were associated with extracellular field recordings (26). (*D*) (*Left*) Each dot indicates a synchronized inhibitory event (giant inhibitory postsynaptic potential) in the presence of 4-aminopyridine (4-AP), (*R,S*)-3-(2-carboxypiperazin-4-yl)propyl-1-phosphonic acid (CPP), and 6-cyano-7-nitroquinoxaline-2,3-dione (CNQX). (*Right*) Expanded traces recorded at −45 mV showing typical triphasic synchronized giant inhibitory postsynaptic potentials recorded in PLC-$\beta1^{+/+}$ (n = 10) and PLC-$\beta1^{-/-}$ (n = 10) slices. The giant inhibitory postsynaptic potential could be recorded simultaneously in pairs of cells and was associated with extracellular field recordings (29–30). Spontaneous action potentials were clipped by digitization.

Lack of Carbachol-Induced Oscillations in the PLC-$\beta1^{-/-}$ Hippocampal Slices. Activation of mGluRs and muscarinic acetylcholine receptors generates stereotyped network oscillations in hippocampal slices that may be important during hippocampal oscillatory states and during uncontrolled epileptiform activities *in vivo* (16, 17, 26, 27). Recently, we demonstrated that group I mGluR-dependent oscillations are abolished in the hippocampus of PLC-$\beta1^{-/-}$ mice (25). Therefore, we examined whether hippocampal slices from PLC-$\beta1^{-/-}$ mice can generate carbachol-induced oscillations by using intracellular recording techniques as described in *Materials and Methods*. In CA3 pyramidal cells of wild-type slices, bath application of carbachol at 15 μM induced synchronized oscillations of 9 Hz with a reversal potential of approximately −70 mV, approximating the equilibrium potential for chloride (n = 14) (Fig. 1*A*, +/+) (cf. ref. 28). Changes in the membrane potential of the recorded cells through intracellular current injection did not affect the frequency of the carbachol-induced oscillations, suggesting that these oscillations were population events. In stark contrast, no such oscillatory activity was generated in the PLC-$\beta1^{-/-}$ slices under the same conditions (n = 7) (Fig. 1*A*, −/−). Treatment with carbachol for longer than an hour still failed to elicit any oscillatory activity in

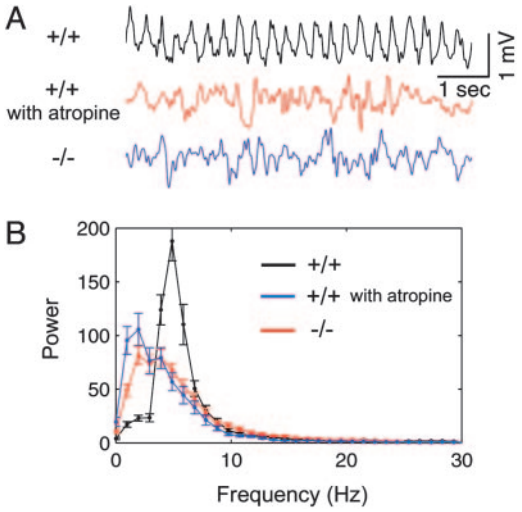

Fig. 2. Absence of *in vivo* urethane-induced theta rhythm in PLC-$\beta1^{-/-}$ mice. (*A*) (*Top*) *In vivo* urethane-induced theta rhythms recorded from the hippocampal fissure of a wild-type mouse. (*Middle*) Atropine suppressed the urethane-induced theta rhythms in the wild-type mouse. (*Bottom*) Urethane failed to induce theta rhythms in the PLC-$\beta1^{-/-}$ mouse hippocampal fissure. (*B*) Average power spectrum of hippocampal EEGs. Here the *x* axis represents EEG frequency scale at a 1-Hz bin width, and the *y* axis represents values of spectral power in relative units (see *Materials and Methods*). Symbols and vertical bars are means and SEMs, respectively. The plots show a peak at theta frequency (5 Hz) in wild-type mice (black plot; $n = 4$) that was blocked by 50 mg/kg i.p. atropine (blue plot, $n = 4$) and was absent in the PLC-$\beta1^{-/-}$ hippocampus (red plot; $n = 4$).

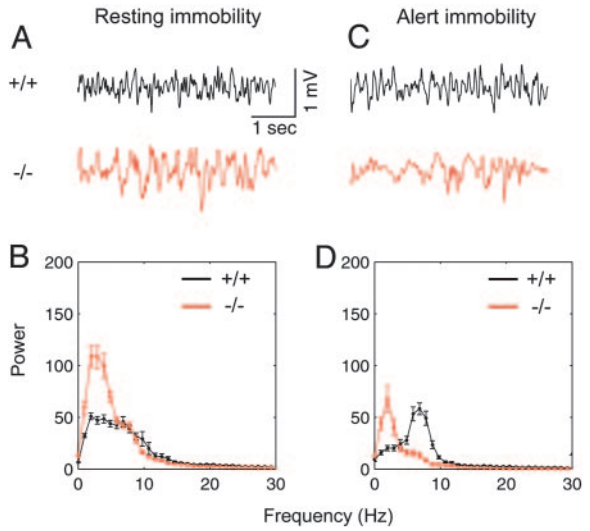

Fig. 3. Hippocampal EEG and power spectra for wild-type and PLC-$\beta1^{-/-}$ mice during resting immobility and alert immobility. (*A*) Representative EEG waveforms during resting immobility (offline digital-filtered in a bandwidth of ≈1–30 Hz) for wild-type mice (+/+) and PLC-$\beta1^{-/-}$ mice (−/−). (*B*) Averaged power spectra of the EEG waveforms recorded during resting immobility for wild-type mice (black plots, $n = 7$) and PLC-$\beta1^{-/-}$ mice (red plots, $n = 7$). (*C*) Representative EEG waveforms during alert immobility for wild-type mice (black trace) and PLC-$\beta1^{-/-}$ mice (red trace). (*D*) Averaged power spectra of the EEG waveforms recorded during alert immobility for wild-type mice ($n = 7$) and PLC-$\beta1^{-/-}$ mice ($n = 7$).

PLC-$\beta1^{-/-}$ slices, indicating that the lack of response was not time-dependent. Furthermore, whereas changes in carbachol dosage modulated the characteristics of carbachol-induced oscillations in the wild-type slices (Fig. 1*B*, +/+), the PLC-$\beta1^{-/-}$ slices did not generate any oscillatory activity under the same conditions (Fig. 1*B*, −/−).

To test the possibility that the oscillation defect in the presence of carbachol resulted from a general defect of hippocampal networks in the PLC-$\beta1^{-/-}$ hippocampus, we examined two other types of population rhythmic activities in the PLC-$\beta1^{-/-}$ hippocampal slices. One type of rhythmic activity was the interictal discharges that were generated through recurrent excitations among pyramidal cells in the presence of picrotoxin (Fig. 1*C*) (cf. ref. 26). The other type of rhythmic activity was the synchronized giant inhibitory postsynaptic potentials that were maintained by connections between inhibitory interneurons and elicited in the presence of the K^+ channel blocker 4-aminopyridine and of the ionotropic GluRs antagonists 6-cyano-7-nitroquinoxaline- 2,3-dione and (*R*,*S*)-3-(2-carboxypiperazin-4-yl)propyl-1-phosphonic acid (Fig. 1*D*) (cf. refs. 29 and 30). Both types of the rhythmic activities were intact in the PLC-$\beta1^{-/-}$ hippocampus. Thus, the oscillation defect in the PLC-$\beta1^{-/-}$ mutation appears to be specific to the cholinergic system rather than being due to a generalized network deficit.

Lack of Urethane-Induced Theta Rhythms in PLC-$\beta1^{-/-}$ *in Vivo*. As a first step to characterize theta rhythms *in vivo* in mutant mice, we performed hippocampal EEG recordings of mice that were anesthetized with urethane. This procedure is known to induce isolated atropine-sensitive theta rhythms mediated via muscarinic acetylcholine receptors (14). In wild-type mice, the urethane-induced theta rhythms recorded in the hippocampal fissure were robustly induced intermittently while the mice were left untouched or continuously during tail pinching (Fig. 2*A*, +/+). These oscillations were disrupted by a subsequent administration of atropine at 50 mg/kg (Fig. 2*A*, +/+ with atropine), confirming that they were atropine-sensitive theta rhythms (cf. ref. 14). In contrast, PLC-$\beta1^{-/-}$ mice under the same conditions showed slow irregular activities in the EEG (Fig. 2*A*, −/−) that appear similar to the EEG pattern observed in wild-type mice after atropine treatment. Averaged power spectra confirmed that urethane-induced theta

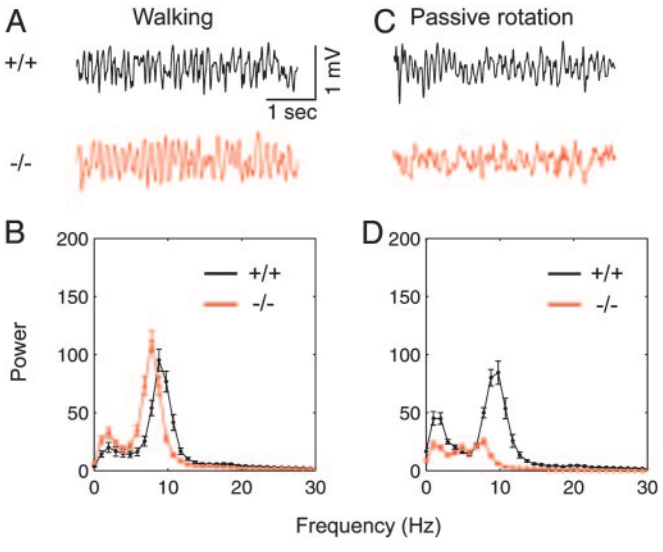

Fig. 4. Hippocampal EEG and power spectra for wild-type and PLC-$\beta1^{-/-}$ mice during walking and passive whole-body rotation. (*A*) Representative EEG waveforms during walking for wild-type mice (+/+) and PLC-$\beta1^{-/-}$ mice (−/−). (*B*) Averaged power spectra of the EEG waveforms recorded during walking for wild-type mice ($n = 7$) and PLC-$\beta1^{-/-}$ mice ($n = 7$). (*C*) Representative EEG waveforms during whole-body passive rotation for wild-type mice (black trace) and PLC-$\beta1^{-/-}$ mice (red trace). (*D*) Averaged power spectra of the EEG waveforms recorded during whole-body passive rotation for wild-type mice ($n = 7$) and PLC-$\beta1^{-/-}$ mice ($n = 7$).

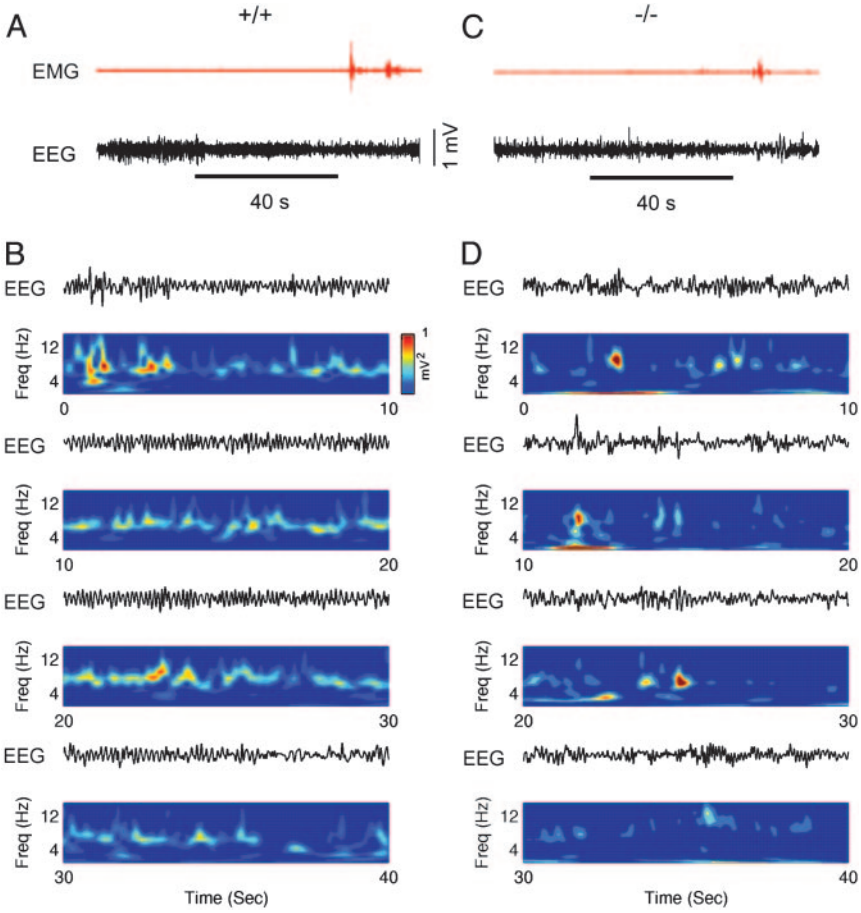

Fig. 5. EEG, EMG, and wavelet time-frequency analysis during paradoxical sleep for wild-type and PLC-$\beta1^{-/-}$ mice. (*A*) Representative EEG and EMG waveforms recorded during slow wave sleep and paradoxical sleep for a wild-type littermate mouse. (*B*) Morlet wavelet transform of a EEG waveform selected for 40 s during paradoxical sleep in a wild-type littermate mouse. Color contour represents the level of wavelet power, where color coding is blue for values close to zero and red for those close to maximum. (*C*) Representative EEG and EMG waveforms recorded during slow wave sleep and paradoxical sleep for a PLC-$\beta1^{-/-}$ mouse. (*D*) Wavelet time-frequency representation of a EEG waveform selected for 40 s during paradoxical sleep in the PLC-$\beta1^{-/-}$ mice. Similar results were observed in four wild-type and four PLC-$\beta1^{-/-}$ mice.

rhythms from wile-type littermates ($n = 4$) were blocked by atropine (50 mg/kg, i.p.) and were absent in the PLC-$\beta1^{-/-}$ hippocampus ($n = 4$) (Fig. 2*B*). Thus, the generation of the urethane-induced theta rhythm *in vivo* was disrupted in the PLC-$\beta1^{-/-}$ hippocampus.

EEG Analysis of PLC-$\beta1^{-/-}$ Mice During Various Behaviors. To investigate the relationships between theta rhythm heterogeneity and behaviors based on a theoretical framework (3), we examined hippocampal EEG in PLC-$\beta1^{-/-}$ and wild-type littermates under five behavioral conditions as described in *Supporting Text*: resting immobility, alert immobility, walking and wheel-running, passive whole-body rotation, and paradoxical sleep.

Resting-Immobility State. Large irregular activity has been more frequently observed during the resting-immobility state, whereas atropine-sensitive theta rhythms can be observed when the animals are alerted by sensory stimulations (1). To compare large irregular activity between PLC-$\beta1^{-/-}$ mice and wild-type littermates, hippocampal electrical activities were recorded while mice were resting (Fig. 3*A*). PLC-$\beta1^{-/-}$ mice showed an increase in the spectral power amplitude at the frequency band of 1–5 Hz during resting-immobile states compared with wild-type littermates ($P < 0.05$, Student's t test) (Fig. 3*B*). This result is consistent with previous reports suggesting that rats show increased low-frequency hippocampal EEG power after muscarinic antagonist administration (31).

Alert-Immobility State. Atropine-sensitive theta rhythms have been often observed during an alert-immobility state (1, 3). To investigate the status of such theta rhythms in mutant mice, we recorded EEGs from PLC-$\beta1^{-/-}$ mice and wild-type littermates under the conditions that would normally induce an alert-immobility state in the mouse. Alert-immobility states were induced by infrequent and random tone stimuli (see *Supporting Text*) (cf. refs. 32 and 33). Theta rhythms appeared when the wild-type mice were sitting motionless and were alerted by infrequent tone stimuli (Fig. 3*C*, $+/+$). In contrast, no theta rhythm was observed in the PLC-$\beta1^{-/-}$ mice under the same experimental conditions rendered by infrequent tones (Fig. 3*C*, $-/-$). The averaged power spectra showed that PLC-$\beta1^{-/-}$ mice did not produce theta rhythms under the conditions that induced alert immobility and robust theta rhythms in wild-type littermates (Fig. 3*D*). Interestingly, the relative EEG power spectral density values in the range of 1–4 Hz computed during alert-immobility states (Fig. 3*D*, red line) were smaller than those computed during resting-immobility states (Fig. 3*B*, red line) in PLC-$\beta1^{-/-}$ mice ($P < 0.05$, Student's t test). These results suggest that the PLC-$\beta1^{-/-}$ mutation changed the characteristics of EEG activity but failed to generate the theta rhythms during alert-immobility states.

Walking. Locomotion, such as walking and running, is accompanied by atropine-resistant theta rhythms (1–3, 13, 14). To confirm whether theta rhythms during locomotion are intact in PLC-$\beta1^{-/-}$ mice, we recorded hippocampal electrical activity while mice were walking. Fig. 4*A* shows that wild-type littermates and PLC-$\beta1^{-/-}$ mice produced theta rhythms during walking. The maximum EEG power in the theta band of 4–12 Hz did not significantly differ between PLC-$\beta1^{-/-}$ mice and wild-type littermates ($P > 0.3$, Student's t test) (Fig. 4*B*). However, the mean theta frequency (7.53 ± 0.13 Hz) at the maximum theta power in PLC-$\beta1^{-/-}$ mice was slightly lower than that (8.78 ± 0.15 Hz) in wild-type littermates ($P < 0.05$, Student's t test).

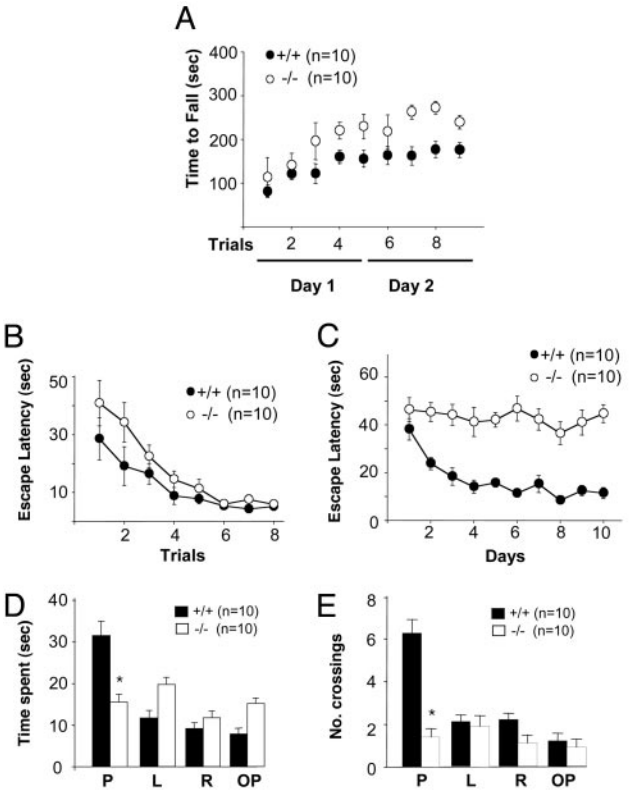

Fig. 6. Behavioral analyses of PLC-$\beta1^{-/-}$ mice and wild-type littermates. (*A*) Time taken to fall from the rotating rod was recorded during five training trials performed within a day and four probe trials performed the next day. PLC-$\beta1^{-/-}$ mice showed enhanced motor coordination. (*B*) Visual cue version of the Morris water maze with eight blocks of trials (four trials per block) and a randomly located platform visualized by a black cylinder (diameter, 5 cm; height, 4 cm). Escape latency is expressed as the time in seconds required to find the platform. (*C*) Spatial task with a hidden platform under the water surface. (*D*) Probe test without a platform. Time spent at four quadrants: P, where the platform had been located; L, left quadrant; R, right quadrant; OP, opposite from where the platform had been located. (*E*) Probe test for accuracy: number of crossings at the location of the platform. Filled symbols and bars represent data from wild-type mice ($n = 10$) and open symbols and bars data from PLC-$\beta1^{-/-}$ mice ($n = 10$).

Passive Whole-Body Rotation. Theta rhythms observed during passive whole-body rotation were shown to be abolished by atropine sulfate (J.S., unpublished data). Therefore, we recorded EEG from PLC-$\beta1^{-/-}$ mice and wild-type littermates while mice were restrained and rotated passively on a turntable. Fig. 4*C* shows that PLC-$\beta1^{-/-}$ mice did not produce theta rhythms during passive rotations (red trace), whereas wild-type littermates did (black trace). During passive rotations, PLC-$\beta1^{-/-}$ mice failed to produce a spectral peak in the theta band (4–12 Hz) greater than that in the delta band (1–4 Hz) (Fig. 4*D*, red plot), whereas wild-type littermates did (Fig. 4*D*, black plot). Similar data were obtained for clockwise and counterclockwise rotations.

Paradoxical Sleep. Atropine-treated rats were shown to display a spontaneous waxing and waning alternation in theta amplitude interrupted by periods of irregular activity during paradoxical sleep (rapid eye movement sleep), indicating that atropine-sensitive and atropine-resistant theta rhythms coexisted during paradoxical sleep (34). Therefore, we analyzed theta rhythms recorded during paradoxical sleep in wild-type and PLC-$\beta1^{-/-}$ mice (Fig. 5). Theta rhythms of wild-type mice were regular and continuous for tens of seconds during paradoxical sleep (Fig. 5*B*), whereas PLC-$\beta1^{-/-}$ mice theta rhythms were intermittent and interrupted by irregular activity between induced theta rhythms (Fig. 5*D*). These results are consistent with previous observations that the atropine-resistant component of theta rhythms appeared during paradoxical sleep of atropine-treated rats (34).

Behavioral Analysis of PLC-$\beta1^{-/-}$ Mice. We next investigated the effects of selective loss of the PLC-$\beta1$-dependent theta rhythm on PLC-$\beta1^{-/-}$ mice behavior (for detailed methodology, see *Supporting Text*). First, we carried out the rotating rod test to examine balance and motor coordination performance. During the first two trials, no difference was observed between the two mouse groups. However, after three trials, PLC-$\beta1^{-/-}$ mice exhibited significantly higher performance scores compared with wild-type mice (Fig. 6*A*). Four more trials performed 24 h later confirmed that the motor learning ability of PLC-$\beta1^{-/-}$ mice was significantly better than that of wild-type littermates ($F(1, 13) = 291.402$, $P < 0.001$, ANOVA for genotype).

Second, we performed the Morris water maze test to investigate whether PLC-$\beta1^{-/-}$ mice had spatial learning deficits. In the visual cue version of the Morris water maze, which is a hippocampus-independent task, no significant difference was noted in overall performance between the two mouse groups (Fig. 6*B*). However, in the hippocampus-dependent hidden platform version of the test, PLC-$\beta1^{-/-}$ mice showed a severe learning deficit compared with wild-type mice (Fig. 6*C*). No decrease in escape latency was observed over 10 days of trials ($F = 96.618$, $P < 0.0001$, ANOVA) (Fig. 6*C*). In probe tests, whereas wild-type mice preferentially spent their time swimming in the pool quadrant where the platform had been located during training, PLC-$\beta1^{-/-}$ mice showed no such preference (PLC-$\beta1^{+/+}$, $P < 0.005$; PLC-$\beta1^{-/-}$, $P > 0.2$; paired Student's t test for place) (Fig. 6*D*). Additionally, in this probe trial, PLC-$\beta1^{-/-}$ mice crossed over the exact location of the hidden platform significantly fewer times compared with wild-type littermates (PLC-$\beta1^{+/+}$, $P < 0.005$; PLC-$\beta1^{-/-}$, $P > 0.3$; paired Student's t test for place) (Fig. 6*E*).

Discussion

Based on data obtained by using PLC-$\beta1^{-/-}$ mice, this report clearly demonstrates that theta rhythms can be divided into two subgroups: PLC-$\beta1$-dependent and PLC-$\beta1$-independent. The lack of urethane-induced theta rhythms in PLC-$\beta1^{-/-}$ mice and the lack of carbachol-induced oscillations in PLC-$\beta1^{-/-}$ mice hippocampal slices, together with the similarities between PLC-$\beta1^{-/-}$ mice and atropine-treated animals regarding theta rhythms generated during walking (14), alert immobility (1), passive rotation (J.S., unpublished data), and paradoxical sleep (34), suggest the existence of PLC-$\beta1$-dependent and PLC-$\beta1$-independent forms of theta rhythms reminiscent to atropine-sensitive and atropine-resistant forms of theta rhythm, respectively. Given that PLC-$\beta1$ is coupled to three muscarinic acetylcholine receptors (M1, M3, and M5) via the α subunit of G_q proteins (22), the present data indicate that, despite the existence of multiple muscarinic receptors and the diversity of their downstream signal pathways, the generation of atropine-sensitive theta rhythm in the hippocampus is mediated by the muscarinic acetylcholine receptor (M1, M3, and/or M5)-$G_{\alpha q}$-PLC-$\beta1$-dependent pathway. Among muscarinic receptors M1, M3, and M5, M1 is especially predominant in the hippocampus and is expressed in the pyramidal cell bodies and apical and basal dendrites of the stratum radiatum and stratum oriens (35). Taken together, it is expected that the M1-$G_{\alpha q}$-PLC-$\beta1$-dependent pathway in hippocampal pyramidal cell bodies and dendrites is critically involved in the atropine-sensitive component of theta rhythm. Consistent with this prediction, it has been shown that the M1-selective muscarinic antagonist pirenzepine blocks carbachol theta-like oscillation in hippocampal slices (36) and atropine-sensitive theta rhythm *in vivo* (37).

The neurotransmitter involved in the generation of the atropine-resistant theta rhythm remains unclear. Contribution of GluRs has

been suggested. In particular, the involvement of NMDA receptors has been emphasized based on the observation that 2-amino-5-phosphonovaleric acid abolished the atropine-resistant theta rhythm *in vivo* (11). However, the exclusive involvement of NMDA receptors is in question. Leung and Desborough (38) proposed that, although 2-amino-5-phosphonovaleric acid suppressed the atropine-resistant theta rhythm, it was more potent against the atropine-sensitive component of theta rhythm. Group I mGluRs generate population oscillations in the hippocampus *in vitro* (16, 25) and may be involved in sustaining atropine-resistant theta rhythm. However, our data reveal that group I mGluR-dependent oscillations are abolished in the hippocampus of PLC-$\beta1^{-/-}$ mice (25). The present finding that the atropine-resistant rhythm persists in this mutant mouse suggests that the generation of this rhythm may not depend on group I mGluRs. In addition to group I mGluRs, glutamate also stimulates group II and group III mGluRs, receptors that down-regulate adenylyl cyclase and mediate presynaptic inhibition. It is unlikely that group II and group III mGluRs can sustain theta oscillations because their action is mainly inhibitory and indeed has been shown to suppress epileptiform population oscillations (39, 40). In addition, it was suggested that the interaction between GABAergic neurons in the medial septum and GABAergic interneurons in the hippocampus may be important for the atropine-resistant theta rhythm (12). Thus, available data suggest that the atropine-resistant theta rhythms may result from the concerted actions of different neurotransmitters on various brain regions.

In contrast, it has long been discussed whether carbachol-induced theta-like oscillation *in vitro* is closely related to *in vivo* atropine-sensitive theta rhythm (1, 11–14, 17, 36). Interestingly, PLC-$\beta1$ is predominantly expressed in the hippocampus but is not expressed in the medial septum (24). Therefore, the present results indicate that the cholinergically induced oscillations observed in hippocampal slices share, at least in part, the same signaling mechanism with the PLC-$\beta1$-dependent theta rhythms recorded *in vivo*. What is then the downstream target of PLC-$\beta1$ involved in the genesis of carbachol oscillation and atropine-sensitive theta rhythm *in vivo*? The biophysical effects of carbachol have been studied extensively. These effects include suppression of three separate K^+ conductances (the voltage- and time-dependent K^+ current I_M, the slow Ca^{2+}-activated K^+ current I_{AHP}, and the time- and voltage-independent leakage K^+ current) (41) and potentiation of two mixed cation currents (the hyperpolarization-activated current I_h and a Ca^{2+}-dependent, nonspecific cation conductance, I_{cat}) (42). Recent evidence has demonstrated that M1 receptors selectively modulate the two mixed cation conductances (I_h and I_{cat}) without affecting hippocampal potassium conductance (43). In general, hyperpolarization-activated cation currents (I_h) have been suggested to influence network oscillations that may play important roles in learning and memory (44–46). Recent studies demonstrated that I_h current is involved in modulating theta rhythm *in vivo* (47–49). Interestingly, Cobb *et al.* (27) demonstrated that, at concentrations that fully block I_h, the I_h inhibitor ZD7288 abolishes muscarinic acetylcholine receptor- and mGluR-induced theta-based oscillatory activity in hippocampal slices (27). However, it should be noted that the I_h inhibitor ZD7288 also reduces $GABA_A$ receptor-mediated postsynaptic responses (see ref. 16). Furthermore, it is not yet clear whether h-channels expressed in the hippocampal pyramidal neurons may be critically involved in the genesis of atropine-sensitive theta rhythm *in vivo* (47–49). Therefore, further studies are necessary to investigate the cell-type-specific downstream pathways involved in cabarchol-induced oscillations *in vitro* and in the atropine-sensitive theta rhythm *in vivo*.

Interestingly, PLC-$\beta1^{-/-}$ mice showed normal spatial learning under a visual platform version of the Morris water maze but showed deficit under a hidden platform version of the Morris water maze. In contrast to its negative effect on spatial cognition, PLC-$\beta1$ mutation did not adversely affect (and indeed improved) motor coordination and motor learning as assayed with the rotarod test. These findings suggest that the atropine-sensitive component of theta rhythm may not be necessary for motor coordination and motor learning in the rotarod test, although a possibility still exists that a developmental compensation occurred for the deficit of PLC-$\beta1$ in the motor regulation pathways.

Theta rhythm is a major endogenous signal in the brain (3). Therefore, future studies regarding hippocampal functions or dysfunctions, such as schizophrenia, epilepsy, and Alzheimer's disease, will have to take into considerations the hippocampal theta rhythm heterogeneity.

This work was supported by the Korea Institute of Science and Technology, the Korea Science and Engineering Fund, and the National Institutes of Health.

1. Bland, B. H. (1986) *Prog. Neurobiol.* **26,** 1–54.
2. Shin, J. & Talnov, A. (2001) *Brain Res.* **897,** 217–221.
3. Shin, J. (2002) *Biosystems* **67,** 245–257.
4. Tesche, C. D. & Karhu, J. (1999) *J. Cognit. Neurosci.* **11,** 424–436.
5. Vertes, R. P. & Kocsis, B. (1997) *Neuroscience* **81,** 893–926.
6. Raghavachari, S., Kahana, M. J., Rizzuto, D. S., Caplan, J. B., Kirschen, M. P., Bourgeois, B., Madsen, J. R. & Lisman, J. E. (2001) *J. Neurosci.* **21,** 3175–3183.
7. Kunec, S., Hasselmo, M. & Kopell, N. (2005) *J. Neurophysiol.* **94,** 70–82.
8. Wyble, B. P., Hyman, J. M., Rossi, C. A. & Hasselmo, M. E. (2004) *Hippocampus* **14,** 662–674.
9. O'Keefe, J. & Nadel, L. (1978) *The Hippocampus as a Cognitive Map* (Oxford Univ. Press, New York).
10. Winson, J. (1978) *Science* **201,** 160–163.
11. Buzsáki, G. (2002) *Neuron* **33,** 325–340.
12. Stewart, M. & Fox, S. E. (1990) *Trends Neurosci.* **13,** 163–168.
13. Leung, L. S. (1998) *Neurosci. Biobehav. Rev.* **22,** 275–290.
14. Kramis, R., Vanderwolf, C. H. & Bland, B. H. (1975) *Exp. Neurol.* **49,** 58–85.
15. Vertes, R. P. (1986) *In The Hippocampus*, eds. Isaacson, R. L. & Pribram, K. H. (Plenum, New York), Vol. 4.
16. Gillies, M. J., Traub, R. D., LeBeau, F. E., Davies, C. H., Gloveli, T., Buhl, E. H. & Whittington, M. A. (2002) *J. Physiol.* **543,** 779–793.
17. Konopacki, J., MacIver, M. B., Bland, B. H. & Roth, S. H. (1987) *Brain Res.* **405,** 196–198.
18. Exton, J. H. (1996) *Ann. Rev. Pharmacol. Toxicol.* **36,** 481–509.
19. Nishizuka, Y. (1988) *Nature* **334,** 661–665.
20. Abe, T., Sugihara, H., Nawa, H., Shigemoto, R., Mizuno, N. & Nakanishi, S. (1992) *J. Biol. Chem.* **267,** 361–368.
21. Gutkind, J. S., Novotny, E. A., Brann, M. R. & Robbins, K. C. (1991) *Proc. Natl. Acad. Sci. USA* **88,** 4703–4707.
22. Rhee, S. G. & Bae, Y. S. (1997) *J. Biol. Chem.* **272,** 15045–15048.
23. Kim, D., Jun, K. S., Lee, S. B., Kang, N. G., Min, D. S., Kim, Y. H., Ryu, S. H., Suh, P. G. & Shin, H. S. (1997) *Nature* **389,** 290–293.
24. Watanabe, M., Nakamura, M., Sato, K., Kano, M., Simon, M. I. & Inoue, Y. (1998) *Eur. J. Neurosci.* **10,** 2016–2025.
25. Chuang, S. C., Bianchi, R., Kim, D., Shin, H. S. & Wong, R. K. (2001) *J. Neurosci.* **21,** 6387–6394.
26. Traub, R. D. & Wong, R. K. (1982) *Science* **216,** 745–747.
27. Cobb, S. R., Larkman, P. M., Bulters, D. O., Oliver, L., Gill, C. H. & Davies, C. H. (2003) *Neuropharmacology* **44,** 293–303.
28. Bland, B. H., Colom, L. V., Konopacki, J. & Roth, S. H. (1988) *Brain Res.* **447,** 364–368.
29. Aram, J. A., Michelson, H. B. & Wong, R. K. (1991) *J. Neurophysiol.* **65,** 1034–1041.
30. Michelson, H. B. & Wong, R. K. (1991) *Science* **253,** 1420–1423.
31. Leung, L. S. (1985) *Electroencephalogr. Clin. Neurophysiol.* **60,** 65–77.
32. Shin, J., Lu, B. L., Talnov, A., Matsumoto, G. & Brankack, J. (2001) *Neurocomputing* **38,** 1557–1566.
33. Lu, B. L., Shin, J. & Ichikawa, M. (2004) *IEEE Trans. Biomed. Eng.* **51,** 551–558.
34. Robinson, T. E., Kramis, R. C. & Vanderwolf, C. H. (1977) *Brain Res.* **124,** 544–549.
35. Volpicelli, L. A. & Levey, A. I. (2004) *Prog. Brain Res.* **145,** 59–66.
36. Williams, J. H. & Kauer, J. A. (1997) *J. Neurophysiol.* **78,** 2631–2640.
37. Barnes, J. C. & Roberts, F. F. (1991) *Eur. J. Pharmacol.* **195,** 233–240.
38. Leung, L. W. & Desborough, K. A. (1988) *Brain Res.* **463,** 148–152.
39. Neugebauer, V., Keele, N. B. & Shinnick-Gallagher, P. (1997) *J. Neurosci.* **17,** 983–995.
40. Moldrich, R. X., Chapman, A.G., De Sarro, G. & Meldrum, B. S. (2003) *Eur. J. Pharmacol.* **476,** 3–16.
41. Madison, D. V., Lancaster, B. & Nicoll, R. A. (1987) *J. Neurosci.* **7,** 733–741.
42. Colino, A. & Halliwell, J. V. (1993) *Eur. J. Neurosci.* **5,** 1198–1209.
43. Fisahn, A., Yamada, M., Duttaroy, A., Gan, J. W., Deng, C. X., McBain, C. J. & Wess, J. (2002) *Neuron* **33,** 615–624.
44. Kopell, N. & LeMasson, G. (1994) *Proc. Natl. Acad. Sci. USA* **91,** 10586–10590.
45. Hasselmo, M. E., Fransen, E., Dickson, C. & Alonso, A. A. (2000) *Ann. N.Y. Acad. Sci.* **911,** 418–446.
46. Rotstein, H. G., Pervouchine, D. D., Acker, C. D., Gillies, M. J., White, J. A., Buhl, E. H., Whittington, M. A. & Kopell, N. (2005) *J. Neurophysiol.* **94,** 1509–1518.
47. Nolan, M. F., Malleret, G., Dudman, J. T., Buhl, D. L., Santoro, B., Gibbs, E., Vronskaya, S., Buzsaki, G., Siegelbaum, S. A., Kandel, E. R. & Morozov, A. (2004) *Cell* **119,** 719–732.
48. Kocsis, B. & Li, S. (2004) *Eur. J. Neurosci.* **20,** 2149–2158.
49. Xu, C., Datta, S., Wu, M. & Alreja, M. (2004) *Eur. J. Neurosci.* **19,** 2299–2309.